

Investigation of Fiber Optic-Based-Refractometer for Biogas Sensing

Phairin Thaisongkroh and Saroj Pullteap*

Department of Mechanical Engineering, Faculty of Engineering and Industrial Technology, Silpakorn University, Nakhon Pathom, Thailand

* Corresponding author. E-mail: saroj@su.ac.th DOI: 10.14416/j.asep.2023.03.003

Received: 2 October 2022; Revised: 13 January 2023; Accepted: 13 February 2023; Published online: 16 March 2023

© 2023 King Mongkut's University of Technology North Bangkok. All Rights Reserved.

Abstract

In this study, a fiber-based refractometer (FOR) applied for biogas sensing has been investigated. Two types of fiber, single-mode (SMF) and multimode fiber (MMF) have been proposed as sensing elements. The research aims to investigate the spot and power attenuation of both fiber types in 4 main conditions; fiber cladding, de-cladding, compound coating, and biogas feeding. The experimental results showed that the spot diameters from both fiber types are constantly at 4 and 26 mm in any conditions. This causes the difference in core diameters and also the dispersion of light characteristics within the fibers. Moreover, when the sensing element has been modified by the following conditions, the results indicated that the output intensity has proportionally changed, according to the fiber modification and the concentration of biogas absorbed into the sensing element. Besides, the power attenuation from MMF is larger than SMF. This causes the length of fiber de-cladding and dispersion of light within the MMF can easily be induced by biogas feeding. Therefore, it can be concluded that the MMF is more suitable than SMF for employment as a sensing element of the fiber refractometer.

Keywords: Single-mode fiber, Multi-mode fiber, Sensing element, Fiber optic-based refractometer, Chemical compound, Power attenuation

1 Introduction

Thailand, nowadays, is at a top-five of Southeast Asia in terms of the growth of the agriculture industries and agricultural processes, such as the cattle ranches, sugar industry, paper mills industry, tapioca starch industry, rubber processing industry, etc [1], [2]. However, the operational effects of these industries are reported in stages of draining some wastes into the environment during the manufacturing process, such as wastewater from washing vegetables, bagasse, etc. Besides, these wastes are, directly, pollute the environment, affecting humans, and also animals [3]. To protect against such problems, an organization in Thailand namely the *Department of alternative energy development and efficiency* has, therefore, defined a policy to reproduce industrial waste into renewable energy such as biogas [4]. Furthermore, an annual report from the Ministry of Energy in Thailand described that there are more than

300 biogas plants that currently reproducing industrial wastes into biogas. Moreover, these plants can thus be categorized into seven main groups as summarized in Table 1 [5].

Table 1: Summarization of biogas capacity reproduced by Thailand industries

Industry Types	Biogas Capacity (Mm ³ /y)	Biogas Capacity (in percentage)
Tapioca starch	377	39.95
Alcoholic beverage	110	11.66
Food	100	10.60
Palm	25.3	2.68
Paper	29	3.07
Rubber	84	8.90
Ethanol	218.4	23.14

Generally, biogas is a renewable fuel that usually is reproduced from agricultural or industrial wastes in the stage of the anaerobic digestion process. However,

biogas consists of 55–75% of Methane, (CH_4), Carbon dioxide (CO_2) 25–45%, while Hydrogen sulfide (H_2S), Nitrous oxide (NO_x) are the rest. However, Methane is an important gas that is used for fuelling the vehicle, home cooking, and also generating electricity [6]. To detect or measure the quantity/concentration of gases from the biogas plant, a special instrument namely a “biogas analyzer” has been proposed [7]. However, there are some limitations of the instrument that are exploited in stages of need to operate in-line (on-site) measurement, compulsory to calibrate sensing probe, and unable to measure in real-time [7]. Focusing on in-line measurement cases, this process is very dangerous for the operator's health causing long-term H_2S gas inhaling. To compensate for this stuff, an online biogas analyzer has been proposed. A basic principle of this instrument is a combination between a classical biogas analyzer and a communication module. Even though, online biogas measurement can eliminate the effect as mentioned above. Unfortunately, the problem of the compulsory sensing probe calibration still occurred.

To solve this, the use of a fiber optic sensor (FOS) is the best choice for replacement due to its ability to operate in hazardous areas, high sensitivity, immunity to electromagnetic waves, multiplexing measurements remotely monitored in real-time, etc. [8]. However, the name FOS for gas sensing had first mentioned in the 1980s and has continuously developed up to the present. The examples of the FOS for gas sensing purposes have been reported by Ke *et al.* [9] developed an optical fiber-based evanescent-wave sensing for the hydrogen sulfide gas (H_2S) measurement. The sensor using a technique of evanescent-wave power ratio (EWPR) cooperated with an optical-fiber evanescent wave absorption system (OFWAS) for improving the sensitivity and also stability of the system. Besides, the results showed that the fiber sensor can measure the concentration of H_2S in the range of 45 ppm to 225 ppm with a sensitivity indicated of $\sim 0.169 \mu\text{m/ppm}$. However, this research is more complex to implement, especially the etching process with the SMF. Besides, Renganathan *et al.* developed a fiber gas sensor for toxic gas sensing applications. The sensing mechanism was based on an evanescent wave absorption. The fiber cladding was grazed by using a silicon carbide blade and then coated with tin oxide (SnO_2) for employment as a sensing element to detect toxic gases i.e. Benzene,

Methanol, Ammonia, etc. The results reported that the sensor had a sensitivity to detect the Benzene of 79 counts/100 ppm and to be able to recover itself in 37 min [10]. Furthermore, Zhou *et al.* described an interesting technique for detecting hydrogen sulfide (H_2S) by using the optical fiber Bragg grating (FBG). The Argentum compound (Ag) has been coated onto the fiber cladding for gas detection. The experimental results indicated that the system can absorb the hydrogen sulfide gas with a high sensitivity of 0.33 dBm/percentage, and high linearity obtained [11]. From the articles mentioned above, we realized that single-mode fiber (SMF), and also fiber Bragg grating (FBG) have often been used for developing gas sensing purposes. However, the drawbacks of those fiber types are represented in terms of the complexity to modify fiber cladding causing small core diameter, and also compulsory using a broadband light source cooperated with a special instrument such as the optical spectrum analyzer (OSA) [12].

A fiber optic refractometer (FOR) is a type of FOS that often use the refractive index (RI) of the external medium to predict the desired quantities i.e. chemical analysis, food testing, environmental monitoring, etc. [13]. It is generally classified into three main groups, fiber-based interferometers, grating-based structures, and also resonance-based structures, respectively [14]. The former group is based on the interference between a couple of propagation lights with different paths, sensing and reference signals, recombined to generate the interference signal. The OFWAS also is a part of the optical fiber system. There are several researchers developed the sensor for gas-sensing applications. For example, Wang *et al.* proposed a gas refractometer based on the extrinsic fiber Fabry-Perot interferometer for nitrogen gas detection [15]. The refractive index of nitrogen gas is directly proportional to the wavelength shift obtained from the fiber interferometer. However, the results showed that the developed system can detect the RI changes from the range of 1.00054 to 1.00298 with a sensitivity of 974 RIU/nm. In addition, Fan *et al.* developed an ammonia gas sensor based on the fiber-based Mach-Zehnder interferometer [16]. However, the graphene oxide has been coated at the sensing arm for detecting the ammonia gas (NH_3). Consequently, the results indicated that the proposed system could, perfectly, detect the NH_3 concentration in the range of 0 to 151 ppm with a sensitivity of

4.97 pm/ppm. The second group of FOR uses the optical fiber Bragg grating as a sensing arm to detect physical properties such as displacement, temperature, strain, force, concentrations of gases, etc. [17]. An example of a gas-sensing application is mentioned by Kurohiji *et al.* [18]. They developed the FBG for hydrogen (H_2) gas measurement. Platinum-supported silica (Pt/SiO₂) with an atom ratio between the Si and Pt of 13:1 has been coated onto the grating portion. However, the central wavelength would be shifted according to the concentration of hydrogen gas changed. Further, the experimental results showed that the mentioned sensor can detect hydrogen gas from the concentration of 0.6 vol.% to 3.0 vol.% with a sensitivity of 0.1 vol.%/pm. The latter group of FOR is often used to develop gas sensing. Surface plasmon resonance (SPR), and Lossy mode resonance (LMR) are examples of resonance-based structures. The fiber cladding has been modified and externally coated with some conducting materials such as gold (Au), indium tin oxide (ITO), zinc oxide (ZnO), tin oxide (SnO₂), etc to detect the desired gases [19]. However, this fiber type is more complicated to fabricate, and also the sensitivity of a sensing system is depending on several factors, such as the thickness of fiber de-cladding, the refractive index of the coating material, wavelength operation, etc [20].

In this work, an investigation of a biogas sensing system using a fiber optic-based refractometer (FOR) has, preliminary, been focused. A simple structure and also standard material have been proposed to develop the optical fiber sensor. The sensing mechanism is based on the OFWAS. Further, the sensor structure consists of 3 main parts: light source, sensing element, and photodetection system, respectively. Focusing on the sensing element, two types of optical fiber cords, single-mode fiber (SMF) and multi-mode fiber (MMF) have been proposed to investigate their properties for operating as a sensing element. Spot diameter and light intensity measurements over 4 testing conditions, fiber cladding, de-cladding, chemical coating, and biogas feeding, are the main process of this studying. Besides, Argentum (Ag) has been operated as a compound for detecting/absorbing the desired biogas especially, the hydrogen sulfide gas (H_2S). Further, a photodetector has been used for converting the output light intensity obtained from the element to voltage for data analysis. This signal is, generally, related to the concentration

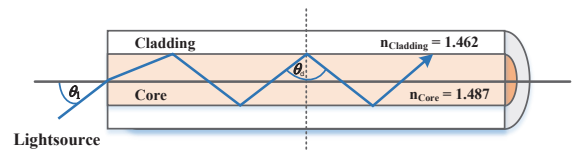


Figure 1: Propagation of light in optical fiber.

of gas absorbed by the chemical compound. However, the highlights of the work are exploited in terms of simple implementation, low cost, not compulsory use of special optical equipment, etc. However, the results would indicate a suitable fiber type that is appropriate to use as a sensing element of the FOR applied for the biogas sensing system.

2 Materials and Methods

The main purpose of this research work is, however, to investigate the physical properties, spot diameter, and power attenuation, of a couple of fiber types, SMF and MMF, which have been used as a sensing element of the fiber refractometer applied for biogas sensing. However, the methods and materials of the work have, consequently, been described below:

2.1 Propagation of light in optical fiber

Optical fiber is a type of transmission media that the light beam has been operated as a carrier to transfer information/signal from one to another. However, its structure is, normally, made from silica or plastic [21]. In addition, the operating principle of such is based on the phenomenon of reflection of light in the difference of refractive index (RI) between the core and cladding within the optical fiber. This phenomenon is, generally, occurred when the RI of the fiber core (n_{core}) is greater than fiber cladding ($n_{cladding}$). However, this concept is illustrated in Figure 1.

Figure 1 shows the light propagated in the optical fiber. However, there is a difference in the RI between the fiber core and cladding. As shown in the figure, the fiber core has a RI value of 1.487, while the cladding is indicated at 1.462, respectively [21]. This leads to the propagation of light within the fiber would not be disturbed along the fiber length. Consequently, this phenomenon is called "Total internal reflection (TIR)". Furthermore, the dispersion of light waves within the optical fiber can, generally, be classified into three

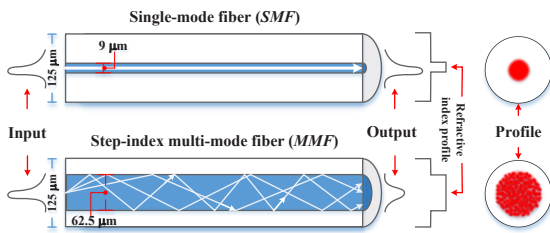


Figure 2: Dispersion of light profiles in single-mode and multi-mode fibers.

main types, single-mode, step-index, and graded index, respectively. In this work, we would only be concerned with the dispersion of light in single-mode (SM) or fundamental mode (FM) and step-index (SI) between the SMF and MMF cords. The dispersion profiles of each fiber type can thus be illustrated in Figure 2.

Figure 2 shows the dispersion of light in a couple of fiber optic types, SMF and MMF. Focusing on the physical property of such fiber, it indicates that a fiber cladding diameter of both fiber types is equivalent to 125 μm , while the core diameter of SMF and MMF is to be 9 μm , and 62.5 μm , respectively. In addition, the numerical aperture (NA) between the SMF and MMF is ~ 0.1 , and ~ 0.2 , respectively. However, this parameter has been used for considering the dispersion of light beams within the fiber [22]. As illustrated in the figure, we realize that the SMF core is very small, leading to a straight line of the emitting light propagated. This phenomenon is, however, signified by a “fundamental mode”. On another hand, the propagated light within the MMF namely “step-index mode”, respectively [22].

2.2 Fiber optic based refractometer

As mentioned before, a fiber optic-based refractometer (FOR) is a classical type of optical instrument that uses a principle of refractive index change (RI) to determine the physical quantities. Consequently, this instrument has, first, been developed more than 2 decades years ago, with several advantages, such as high sensitivity, distinguishing compositions/concentrations of gases, capability to operate in hazardous areas, etc [23]–[25]. However, the principle of FOR is described in terms of the relationship between the changing of a physical quantity and a refractive index within the optical fiber. However, this phenomenon is directly proportional to

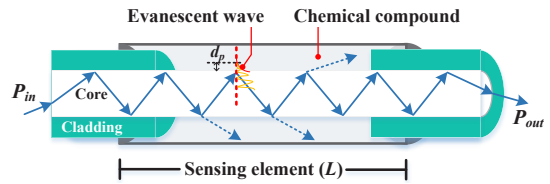


Figure 3: Concept of dispersion of light within fiber refractometer applied for biogas sensing.

the optical power attenuation at the output fiber arm. To design and develop the optical fiber refractometer for biogas sensing, the sensor would have consisted of 3 important parts; light source, sensing element, and photodetection, respectively. A monochromatic light from a laser source has, initially, injected the light into the input fiber arm. This beam is, then, propagated to the sensing element, and then passed to the output arm, respectively. Focusing on the sensing element, it is a measurand portion that is usually employed to detect a physical quantity i.e. the composition/concentration of the desired gases and then exploited in terms of the RI changes. This parameter in particular is changed when the fiber cladding has been modified, for example, fiber de-cladding, or chemical compound coating onto the fiber. This phenomenon also brings a change in the dispersion of light within the optical fiber, due to the changes in the refraction of light in the de-cladding area. In addition, the purposed parameter is conducted to the optical power variation at the output fiber arm. However, the details of the dispersion of light within the fiber refractometer applied for the biogas sensing system can, thus, be shown in Figure 3.

The figure shows a basic concept of dispersion of light within the sensing element of the FOR. Focusing on this portion, it observes that the fiber has been de-cladded until the core, and next coated with a chemical compound instead. This phenomenon is leading to the changes in refractive index (RI), in which the output optical power of the mentioned system (P_{out}) can, thus, be calculated by Equation (1) [26], [27]:

$$P_{out} = P_{in} \cdot \exp(-\zeta L) \quad (1)$$

where: P_{in} corresponds to the input optical power, and ζ represents the attenuation coefficient of evanescent wave between fiber core and cladding, while L is the length of fiber de-cladding, respectively. In addition,

the attenuation coefficient of the evanescent wave can be given by Equation (2):

$$\zeta = RT \tag{2}$$

where: R corresponds to the reflections of light within the optical fiber per unit length, and T is defined as a transmission coefficient of cladding, which is detailed by Equations (3) and (4), respectively.

$$R = \frac{\cot \theta_1}{2a} \tag{3}$$

$$T = \frac{\alpha \lambda (n_{core}) \cos \theta_1}{\pi n_{cc}^2 \cos^2 \theta_{cc} \sqrt{\cos^2 \theta_{cc} - \cos^2 \theta_1}} \tag{4}$$

where: a is core diameter of fiber optic cable
 α is bulk absorption coefficient
 λ is wavelength
 θ_1 is incidence angle of emitting light in optical fiber
 n_{cc} is refractive index of fiber cladding
 θ_{cc} is critical angle value of a chemical compound

By the way, there is an important factor namely the penetration depth (d_p) between the core and cladding has been concerned. This parameter is considered on the evanescent wave in the de-cladding area [28], [29]. Furthermore, it also brought the attenuation of total reflection (ATR) in the optical fiber [30]. Besides, this parameter can be calculated by Equation (5):

$$d_p = \frac{\lambda}{2\pi(n_{co}^2 \sin^2 \theta - n_{cl}^2)^{1/2}} \tag{5}$$

where: n_{co} and n_{cl} represent the refractive index values between the fiber core and cladding within the optical fiber, respectively.

To detect the physical quantities of the desired measurand by using FOR, some chemical compounds have been coated/doped onto the sensing arm of the fiber sensor. However, Argentum (Ag) is an example of a compound that is often used with the FOR for gas sensing applications [9], [11]. It is a type of solid metal that is naturally produced. Besides, this material is, generally, reacted rapidly with hydrogen sulfide (H_2S)

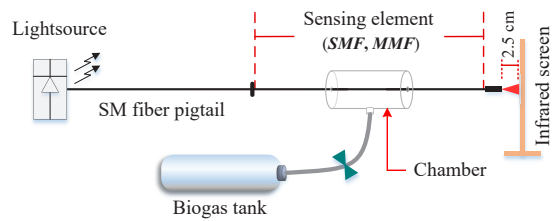


Figure 4: Configuration of spot investigation using fiber optic refractometer.

gas [31]. Therefore, an Ag with a purity of 98.5% has been preliminarily proposed for detecting the hydrogen sulfide gas in this work. However, the objective of Ag usage is not only the capability of its property, but this material is easy to find out at the local place and also not complicated to coat with the fiber.

2.3 Experimental setup

To investigate the physical properties of FOR applied for biogas sensing, 2 fiber types, SMF and MMF, have been concerned as a sensing element. Consequently, the experimental setup has been divided into 2 main parts; spot, and also light intensity measurements in considered conditions such as fiber cladding, fiber de-cladding, compound coating, and biogas feeding. By the way, the process has been followed:

2.3.1 Spot investigation in two optical fiber types

In this experiment, the spot investigations between the SMF and MMF have been demonstrated. There are Four conditions; fiber cladding, fiber de-cladding, chemical compound coating, and biogas feeding have been proposed for studying their properties, and also to justify a suitable fiber type that is appropriate to utilize as a sensing element of the optical fiber refractometer. In addition, there are five times repeatability has been operated in each condition. However, the experimental setup of the proposed system can, thus, be configured in Figure 4.

From Figure 4, monochromatic light from the laser diode source is injected into a single-mode fiber pigtail and then emitted the beam through a sensing element, in which either the SMF or MMF cords have been utilized. However, some portions of the element have been de-cladded and coated with chemical compound and next inserted into a chamber for the

biogas feeding from a biogas tank. Further, the output intensity from the optical fiber end is, then, transmitted to an infrared screen (IR) for observing/measuring the spot diameter, in which the distance between the output fiber end and the IR screen is ~ 2.5 cm. In addition, the spot diameter and spot profiles from both fiber types have, next, been recorded in each experimental condition. However, the experimental results would then investigate a suitable optical fiber cord for employing as a sensing element of the fiber optic-based refractometer.

2.3.2 Light intensity investigation using fiber optic-based refractometer for biogas sensing

This experiment is investigating the properties of FOR to use as a biogas sensor. The experimental process is to measure the output light intensity at the fiber end. However, the experimental setup of this studying can be divided into 3 main parts as followed by:

- *Experiment I* light intensity measurement in fiber cladding condition.
- *Experiment II* light intensity measurement in fiber de-cladding condition.
- *Experiment III* light intensity measurement in fiber coating with a chemical compound condition.

The first experiment is an investigation of the light intensity without modification of the sensing element. In particular, the output light detected by a *Thorlabs* photodetector has, initially, been recorded five times repeatability. This information has, then, been utilized as initial data for data analysis. Moreover, the fiber de-cladding process is next investigated in *Experiment II*. To de-cladding fiber, a hydrofluoric acid (HF) has been proposed. However, there are three steps of such things that have been operated for a fiber de-cladding. The former step is removing the fiber buffer by using an optical fiber stripper. In this work, a fiber cladding length (L) of ~ 1 mm has been removed at the sensing element. Besides, the output profile has been displayed on the microscope SEEK model: SZMN. Consequently, the de-cladding process has, next, been operated by using a 40% concentration of HF. This procedure is called the “etching process” [32]–[34]. It is a process to use an HF to dope into the cladding after removing the buffer. In addition, an important parameter namely the “etching time (ET)” has been concerned. It is the duration time that the fiber cladding

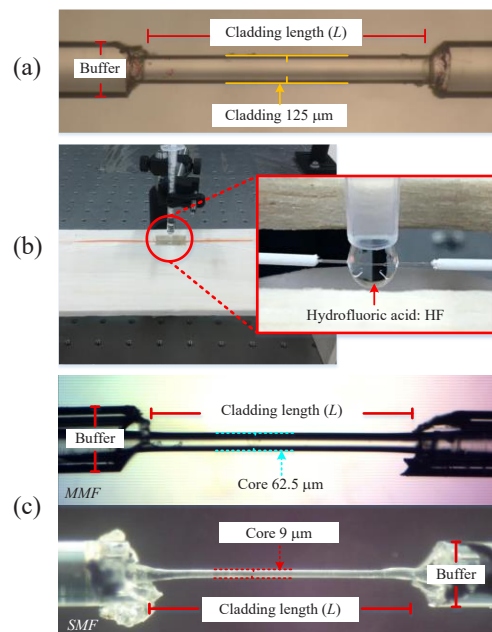


Figure 5: Fiber de-cladding process; (a) removing buffer, (b) HF etching, (c) output from both fiber types.

has been removed until the core. Anyway, the 2 fiber types, SMF and MMF, have been studied in this work. Therefore, there are differences in the etching time between both fiber types, due to the difference in core between both of them. In particular, the SMF would be removed the cladding from $125 \mu\text{m}$ to $9 \mu\text{m}$, while the MMF is eliminated from $125 \mu\text{m}$ to $62.5 \mu\text{m}$, respectively. To obtain this value, the ET of the SMF and MMF cords have been considered at 1.25 h, and 55 min, respectively. After removing the fiber cladding, this portion would, consequently, be coated with a compound instead with a thickness length of 1 mm. However, a procedure of the de-cladding process can be illustrated in Figure 5.

Figure 5(a) and (b) illustrated the process as mentioned above, while Figure 5(c) displayed the output of the etching process from both fiber types, respectively. However, when the fiber cladding has been removed the coating process has, next, been demonstrated. This can investigate in *Experiment III*. In this work, an Ag has been used as a compound to coat onto the sensing element after removing the cladding. As mentioned before, the properties of this compound are utilized to detect biogas especially, the H_2S gas. After completing the process, the sensing

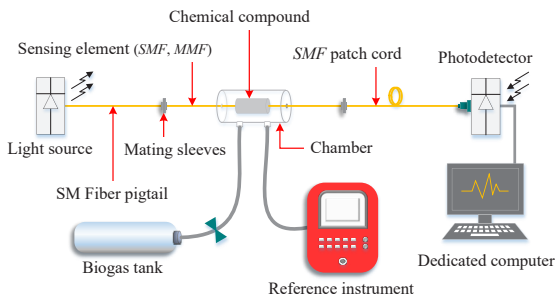


Figure 6: Configuration of the developed system for biogas sensing.

element has been installed into a gas chamber for biogas detection. Remarks that the gases from a biogas tank have, directly, been fed into a chamber, and used only in *Experiment III* after the coating process. The configuration of the experiment can be shown in Figure 6.

According to Figure 6, monochromatic light from the *Thorlabs* model: LPS-1310-FC has, initially, been injected the beam with a wavelength of 1310 nm into a single-mode fiber pigtail, and then emitted the light into the sensing element. Besides, this beam is, next, transmitted into a photodetector (PD) model: PDA10CS from *Thorlabs* to obtain the output intensity. Further, a biogas analyzer model: Biogas 5000 from *Geotech* has been operated as a reference instrument for measuring the concentration of gases from the biogas tank. In this experiment, the gases from the biogas tank included 39.2% of CH_4 , 34.2% of CO_2 , 3.4% of O_2 , and also 700 ppm of H_2S are indicated by the biogas analyzer. These parameters would then be fed into the gas chamber for investigating the properties of the FOR for biogas sensing. The results would, next, be discussed below:

3 Experimental Results and Discussion

As mentioned the setup details in the previous section, the experimental results, and the also discussions have been described in this section, which is followed by:

3.1 Spot investigation of single-mode and multi-mode optical fiber

In this experiment, the spot size and also dispersion of light from SMF and MMF cords in any demonstrated

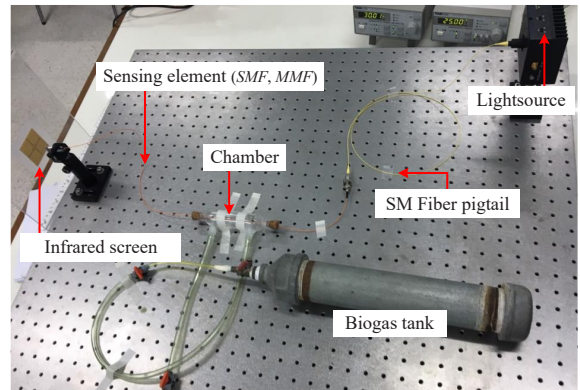


Figure 7: Experimental setup of spot investigation.

conditions as mentioned before have been reported for investigating a suitable optical fiber that would, next, be used as a sensing element of the FOR. However, the results can be described in 4 conditions: fiber cladding, fiber de-cladding, Ag compound coating, and biogas feeding, respectively. However, the actual setup from this experiment can be illustrated in Figure 7.

Figure 7 shows the experimental setup for spot investigation using the optical fiber refractometer. The experimental results in any proposed conditions can, however, be illustrated in Figure 8.

From the figure, we can summarize that the spot diameters between SMF and MMF are, confidentially, equal to 4 and 26 mm in any demonstrated conditions. This implies that the spot from both fiber types would not be perturbed by the physical effects. In addition, we observe that the spot diameter of MMF is always larger than the SMF in any testing condition. This causes the transparent core diameter of the MMF to be larger than the SMF in terms of the physical property, and also the numerical aperture (NA), which the SMF is indicated at 0.14, while 0.22 is exploited from MMF, respectively. Moreover, the spot profile from the SMF is slightly small in size and coherent, while the MMF profile is propagated as a scattering of light. This phenomenon can be verified that the dispersion of light in the SMF is profiled in a single mode, while the step-index mode is obtained by MMF, respectively. Besides, this result is also related to a report work by *Mayeh et al.* [33] that described that the spot diameters of the SMF and MMF were uniform even though the optical fibers had been perturbed, but the spot shapes of both fiber types were changed.

Investigation Conditions	Spot Diameters (mm)		Spot Profiles	
	SMF	MMF	SMF	MMF
Fiber cladding	4	26		
Fiber de-cladding	4	26		
Ag compound coating	4	26		
Biogas feeding	4	26		

Figure 8: Experimental results of spot investigation using fiber refractometer.

3.2 Investigation of light intensity in optical fiber refractometer for biogas sensing

This experiment concerns the output light intensity of the FOR in any conditions as mentioned before. The experimental setup can be illustrated in Figure 9.

Figure 9(a) shows the setup of the biogas sensing using the optical fiber refractometer for investigating the power attenuation under the considered conditions. A configuration of the developed system showed that a monochromatic light from the laser diode source has, directly, been injected into the sensing element which is installed into a biogas chamber. Consequently, the light beam is, next, propagated to a photodetector for measuring the output light intensity in any proposed conditions. Consequently, this light beam is, directly, transferred to a digital oscilloscope by the Tektronix model: TDS2014B for indicating the output intensity in a voltage unit. Moreover, the natural biogas from the biogas tank has been fed into the chamber as a biogas source for validating the performance of the optical fiber refractometer for biogas sensing. In addition, a biogas analyzer from the *Geotech* model: Biogas5000 has also been operated as a reference instrument for detecting the concentration of biogas in a gas chamber. However, the output concentration of gases from the *Geotech* instrument indicated that there are 39.2% of

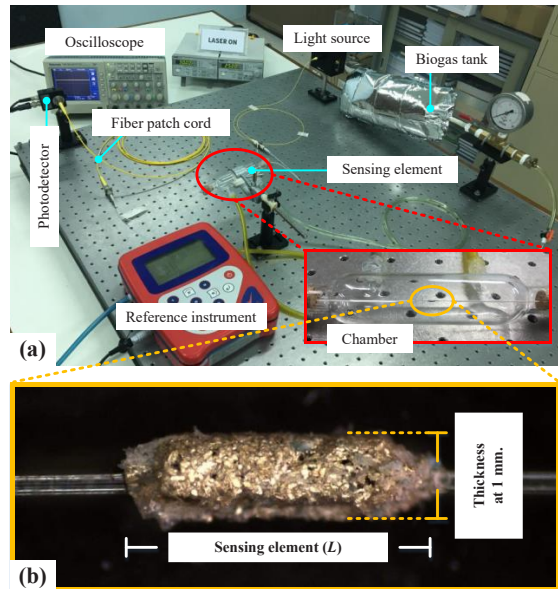


Figure 9: (a) Configuration of the developed system, (b) sensing element coated with Ag compound.

CH_4 , 34.2% of CO_2 , 3.4% of O_2 , and 700 ppm of H_2S fed into the chamber for this demonstration.

In another way, an example of the sensing element coated with an Ag compound and installed in the gas chamber has been illustrated in Figure 9(b). To develop the element, both types of fiber have been de-cladding by the HF and then coated with the Ag compound in a thickness length of 1 mm. However, the main objective to use this compound is for detecting hydrogen sulfide (H_2S) in the system. It causes the H_2S can easily be absorbed by the Ag compound [31]. Furthermore, the advantages of the compound are exploited in terms of easy-to-find, and also shiny appearance for the light reflection, leading to the emitting light within the fiber being penetrated and easily scattered into the element's surface. Besides, this phenomenon has directly related to the change in the optical power at the output of the fiber refractometer. As previously mentioned, there are four experiment conditions have thus been investigated in this research work. Consequently, five times repeatability in each measurement condition has also been concerned to make the reliability of the demonstration results. The average results from each condition have been used for the data analysis. Further, these results can indicate the physical properties of the optical fiber sensor in each

stage of the demonstrated conditions. However, the experimental results from this experiment can thus be summarized in Table 2.

In particular, there are four mainly demonstrated conditions, initial/regular, fiber de-cladding, coating, and biogas feeding, have been investigated its physical properties in this work. However, the results from the table have summarized that the average light intensity obtained from both fiber types in the initial process is indicated of 3.759 V and 3.829 V, respectively. In addition, the standard deviation (Std.) values from both fiber types are exploited of 0.0073, and 0.0335, respectively. This result corresponds to the difference in the fiber core diameter between both fiber cords. Thus, it brought the output intensity achieved from the MMF cord to be significantly larger than SMF. However, please remind that the results are demonstrated in the non-feeding condition only. The next demonstration is a fiber de-cladding process. In particular, the sensing element has been de-cladding at ~1 mm in length and measured the output intensity five times repeatability. The results reported that an average output light intensity has been reduced to 3.564 V and 2.584 V from SMF and MMF with standard deviations archived of 0.015, and 0.0566 respectively. This phenomenon is, however, related to the percentage of power attenuations that are indicated of 5.188% and 32.515% for both fiber types respectively. However, it implies that the output power attenuation would thus be influenced when the sensing element was modified. It causes the scattering of propagation light within the fiber.

To calculate the percentage of a power attenuation (%Att.) from the output intensity in any demonstrated condition, the proposed equation has been given by Equation (6). In particular, this parameter is then used to investigate the ability of the FOR for biogas detection.

$$\%Att. = \left| \frac{I_{reg} - I_{cons}}{I_{reg}} \right| \times 100 \tag{6}$$

where I_{reg} and I_{cons} represented the output intensity in the regular, and considered conditions respectively.

According to the Ag compound coating condition, the output light intensity from both optical fiber types has been achieved of 3.633 V and 2.815 V brought to the standard deviation of 0.0279, and 0.0474 occurred. These results are significantly related to the decrement of the output attenuation from both optical fiber types, which are indicated of 3.352% and 26.48%, respectively. Therefore, we might summarize that the reduction of scattering light within the sensing element is archived when the compound has been coated onto the element.

Consequently, the biogas feeding process has next been concerned. The experimental results showed that when the natural biogas was fed into the biogas chamber, the output intensity from both fiber types are indicated at 3.571 V and 2.710 V with a standard deviation of 0.0074 and 0.0187. These correspond to the increment of output power attenuation between both optical fiber types at 5.001% and 29.224% respectively. Focusing on the percentage of power attenuation from all testing conditions, we might conclude that the highest power attenuation occurred in a stage of the fiber de-cladding process and then slightly decreased when coating with the compound. Consequently, this value was slightly increased when the biogas was directly fed into the gas chamber. This confidentially implies that the biogas could thus be absorbed into the sensing element when the compound has been coated. However, this phenomenon has been summarized in Figure 10.

Table 2: Output intensity in any conditions using a fiber optic refractometer for biogas sensing

Number of Measurements	Initial/Regular Condition		De-cladding Condition		Coating Condition		Gas-feeding Condition	
	SMF	MMF	SMF	MMF	SMF	MMF	SMF	MMF
1	3.76	3.86	3.57	2.66	3.66	2.75	3.58	2.74
2	3.76	3.86	3.56	2.61	3.65	2.79	3.57	2.69
3	3.75	3.80	3.58	2.55	3.62	2.86	3.57	2.71
4	3.77	3.79	3.57	2.59	3.59	2.83	3.56	2.71
5	3.76	3.83	3.54	2.51	3.65	2.85	3.58	2.70
Avg.	3.759	3.829	3.564	2.584	3.633	2.815	3.571	2.710
Std.	0.0073	0.0335	0.0150	0.0566	0.0279	0.0474	0.0074	0.0187
%Att.	0.000	0.000	5.188	32.515	3.352	26.482	0.212	29.224

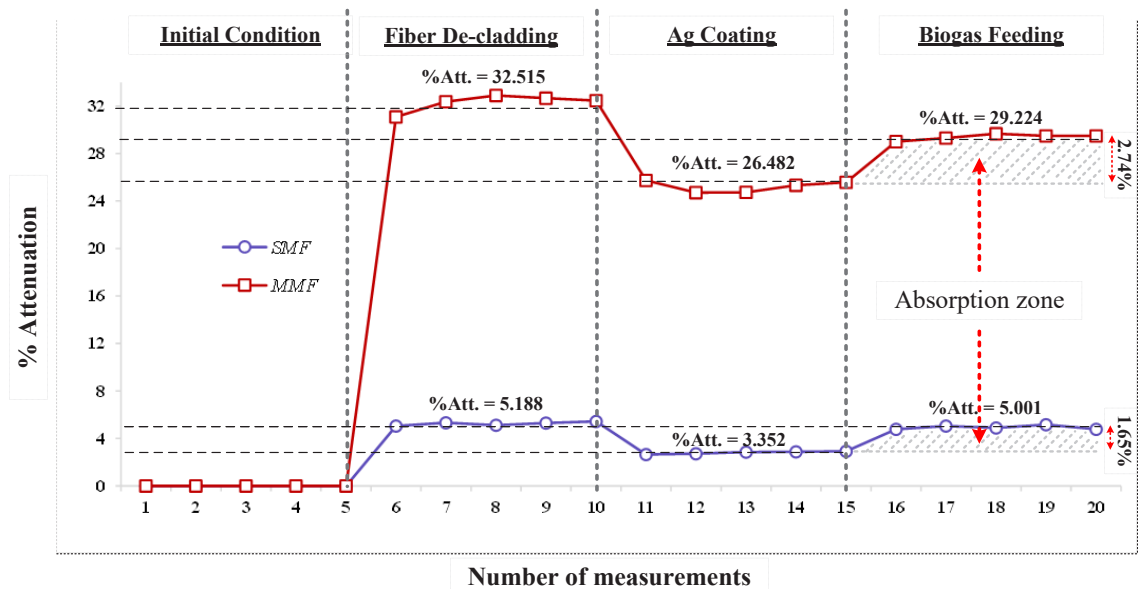


Figure 10: Relationship between number of measurements and power attenuation in any demonstrated conditions obtained output fiber refractometer.

Figure 10 represents the relationship between the number of measurements and power attenuation at the output arm of the refractometer in any demonstrated conditions. However, the results could summarize that the change in power attenuation has been correlated with 3 main factors; type of fiber cord usage, length of fiber de-cladding & coating, and gas feeding process, respectively. In addition, the results were shown that the highest percentage of power attenuation from both fiber types was archived when the fiber cladding was removed. This phenomenon could thus be explained in terms of the scattering of propagation light, and the dispersion of light within the optical fiber. However, this parameter was improved when the compound was coated. Moreover, it would next slightly be increased when the biogas was fed into the sensing element. This implies that the compound was confidently influenced by biogas feeding, leading to the output light intensity being absorbed into the element part. However, these experimental results are related to the results from R. Tan *et al.* [35] which reported that the output power attenuation in a long-period fiber grating (LPFG) was related to the fiber cladding etched. In terms of fiber coating without feeding and with feeding conditions, the results exploited that the difference in percentage attenuation from SMF and MMF cords was indicated at

1.649% and 2.742%. This parameter is corresponding to an absorption capability of biogas from both optical fiber types.

From the results above, it seems that the MMF cord has more significant absorption biogas than SMF. This can be explained in terms of a larger core in diameter and also the dispersion of light within the MMF could easily be induced by the output power attenuation at the coating area. Besides, the attenuation coefficient of the evanescent wave between the fiber core and cladding (ζ) mentioned in Equations (1) and (2) is another important factor to conduct the power attenuation. However, we can prove that the output power (P_{out}) is inversely proportional to the attenuation coefficient of the evanescent wave (ζ) when the input power (P_{in}) and the length (L) of fiber de-cladding are constant. According to the results in Table 2, we observe that the transmission of light (T) in the MMF cord is always larger than the SMF causes of its core diameter as mentioned in Equation (3). However, this brought the attenuation coefficient of the evanescent wave to be bigger than the SMF cord, leading to the output power decrease. This phenomenon is, therefore, related to the results illustrated in Figure 10.

In the case of the coating condition, the results showed a decrement in percentage attenuation from

both fiber types. This phenomenon can be explained in terms of the reflection of light within the coating area as mentioned in Equation (2). It causes the cladding of MMF to be removed/de-cladded at $62.5\ \mu\text{m}$, while SMF is $116\ \mu\text{m}$ respectively. Consequently, it was coated with the Ag compound in a different thickness/layer, leading to the compound density of SMF being denser than the MMF. This phenomenon brought to the reflection of light within the SMF is more reflected than the MMF. However, this result is related to Figure 10, in which the difference in the percentage of power attenuation between the fiber cladding and coating conditions of the SMF cord was indicated as 1.836%, while MMF archived at 6.033% respectively.

According to the results from the feeding process mentioned above, we observe that the MMF cord had more percentage attenuation than the SMF. This result is confidentially correlated to Equation (4) in terms of the bulk absorption coefficient (α) changed due to the biogas absorption into the compound. It brought the variation of the output transmission (T) within the output fiber. From the results in Figure 10, we might thus conclude that the absorption coefficient in the MMF was more coefficient than the SMF, leading to the output power transmission from MMF (T_{MMF}) being bigger than the output transmission from SMF (T_{SMF}). This reason is, consequently, related to the attenuation coefficient of the evanescent wave, and also the output power of the fiber refractometer. As precisely explained above, we might, therefore, summarize that the MMF has more suitable to employ as a sensing element than the SMF for several reasons as mentioned.

4 Conclusions

The investigation of fiber optic-based refractometer (FOR) applied for a biogas sensing system has been studied in this work. Two types of optical fiber cords, SMF and MMF, have been used as a sensing element of the fiber refractometer. The experiments have been concerned with 2 main points; spot profiles, and output power attenuation measurements, respectively. In the first experiment, the results showed that the MMF cord had a larger spot diameter than the SMF. Moreover, the step-indexed dispersion occurred with the MMF, while the single-mode or fundamental mode was in the SMF. This causes the difference in core diameter, and also the dispersion of light within the optical fiber. In the

latter experiment, the results reported that the output power was attenuated when the fiber cladding at the sensing element was modified in any demonstrated conditions. In addition, we observe that the MMF had archived in a higher percentage of power attenuation than the SMF. It causes several reasons such as fiber core diameter, dispersion of light within the fiber, the attenuation coefficient of an evanescent wave between fiber core and cladding, and also the transmission and reflection of light within the optical fiber. Therefore, these imply that the MMF cord was more sensitive and suitable than the SMF regarding physical influential effects. Finally, the results of this research work would be given an idea to develop a prototype of an optical fiber-based refractometer for detecting/measuring the biogas concentration in future work.

Acknowledgments

This research has received funding and support from the Research and Researchers for Industries (RRI), the National Research Council of Thailand (NRCT), and the Realtronics (Thailand) Co., Ltd., through a contract no. PHD62I0035.

Author Contributions

Conceptualization, S.P.; methodology, S.P., and P.T.; validation, S.P., and P.T.; formal analysis, P.T., and S.P.; investigation, P.T., and S.P.; resources, S.P., and P.T.; writing-original draft preparation, P.T., and S.P.; writing-review and editing, P.T., and S.P.; supervision, S.P.; All authors have read and agreed to the published version of the manuscript.

Conflicts of Interest

The authors declare no conflict of interest.

References

- [1] W. Wang, K. Pominta, P. Aggarangsi, N. Leksawasdi, L. Li, X. Chen, X. Zhuang, Z. Yuan, and W. Qi, "Bioenergy development in Thailand based on the potential estimation from crop residues and livestock manures," *Biomass and Bioenergy*, vol. 144, pp. 1–14, 2021.
- [2] P. Soni, "Agricultural mechanization in Thailand:

- Current status and future outlook,” *Agricultural Mechanization in Asia, Africa, and Latin America*, vol. 47, no. 2, pp. 58–66, 2016.
- [3] P. Warr and W. Suphannachart, “Agricultural productivity growth and poverty reduction: Evidence from Thailand,” *Journal Agricultural Economics*, vol. 72, no. 2, pp. 525–546, 2020.
- [4] Ministry of Energy, “Research and development in the field of energy conservation and renewable energy in Thailand”, 2020.
- [5] Report of the Ministry of Energy, “Alternative Energy Development Plan (AEDP2018)”, 2018.
- [6] M. J. B. Kabeyi and O. A. Olanrewaju, “Biogas production and applications in the sustainable energy transition,” *Journal of Energy*, vol. 2022, pp. 1–43, 2022.
- [7] A. J. Calderón and I. González, “Biogas analyzer based on open source hardware: Design and prototype implementation,” *Sensors and Transducers*, vol. 220, no. 2, pp. 31–36, 2018.
- [8] P. Thaisongkroh, P. Samartkit, and S. Pullteap, “Applications of optical fiber sensor technology for prioritized industry in Thailand development strategy: A review,” *Proceedings of SPIE*, vol. 11205, pp. 1120511–1120516, 2019.
- [9] Z. J. Ke, D. L. Tang, X. Lai, Z. Y. Dai, and Q. Zhang, “Optical fiber evanescent-wave sensing technology of hydrogen sulfide gas concentration in oil and gas field,” *Optik*, vol. 157, pp. 1094–1100, 2018.
- [10] B. Renganathan, S. K. Rao, A. R. Ganesan, and A. Deepak, “High proficient sensing response in clad modified ceria doped tin oxide fiber optic toxic gas sensor application,” *Sensors and Actuators A*, vol. 332, Art. no. 11314, 2021.
- [11] H. Zhou, J. Q. Wen, X. Z. Zheng, W. Wang, D. Q. Feng, Q. Wang, and F. Jai, “Study on fiber-optic hydrogen sulfide gas sensor,” *Physics Procedia*, vol. 56, pp. 1102–1106, 2014.
- [12] J. A. F. Bravo, M. A. Illaramendi, J. Zubia, and J. Villatoro, “Optical fiber interferometer for temperature-independent refractive index measuring over a broad range,” *Optics and Laser Technology*, vol. 139, pp. 106977-1–106977-6, 2021.
- [13] A. Ozcariz, C. R. Zamarrino, and F. J. Arregui, “A comprehensive review: Material for the fabrication of optical fiber refractometers based on lossy mode resonance,” *Sensors*, vol. 20, pp. 1–23, 2020.
- [14] M. Yasin, *Fiber Optic Sensor*. London, UK: IntechOpen, pp. 27–52, 2012.
- [15] R. Wang, P. Huang, and X. Qiao, “Gas refractometer based on a side-open fiber optic fabry-perot interferometer,” *Applied Optic*, vol. 56, no. 1, pp. 50–54, 2017.
- [16] X. Fan, S. Deng, Z. Wei, F. Wang, C. Tan, and H. Meng, “Ammonia gas sensor based on graphene oxide-coated mach-zehnder interferometer with hybrid fiber structure,” *Sensor*, vol. 21, pp. 1–13, 2021.
- [17] K. J. Gàsvisk, *Optical Metrology*. London, UK: Wiley & Sons, 2002.
- [18] M. Kurohiji, S. Ichiriyama, N. Yamasaku, S. Okazaki, N. Kasai, Y. Maru, and T. Mizutani, “A robust fiber bragg grating hydrogen gas sensor using platinum-supported silica catalyst film,” *Journal of Sensors*, vol. 2018, pp. 1–9, 2018.
- [19] R. Tabassum and R. Kant, “Recent trends in surface plasmon resonance-based fiber-optic gas sensors utilizing metal oxides and carbon nanomaterials as functional entities,” *Sensors and Actuators B: Chemical*, vol. 310, pp. 1–26, 2020.
- [20] A. Urrutia, I. D. Villar, P. Zubiate, and C. R. Zamarreño, “A comprehensive review of optical fiber refractometers: Toward a standard comparative criterion,” *Laser & Photonics Reviews*, vol. 13, no. 11, pp. 1–32, 2019.
- [21] P. Thaisongkroh, S. Pullteap, and H. C. Seat, “Low-pressure measurement using an extrinsic fiber-based fabry-perot interferometer for industrial applications,” *Engineering Journal*, vol. 25, no. 2, pp. 317–325, 2021.
- [22] A. A. Azzawi, *Fiber Optic: Principles and Advanced Practices*, 2nd Ed. Florida: CRC Press, 2020.
- [23] C. Zhou, W. B. Lee, Y. G. Lee, S. S. Lee, S. H. Son, and B. S. Seol, “Fiber-optic refractometer based on a reflective aspheric prism rendering adjustable sensitivity,” *Journal of Lightwave Technology*, vol. 37, no. 4, pp. 1381–1387, 2019.
- [24] M. F. Churbanov, I. V. Skripachev, G. E. Snopatin, L. A. Ketkova, and V. G. Plotnichenko, “The problems of optical loss reduction in arsenic sulfide glass IR fibers,” *Optical Materials*,

- vol. 102, pp. 1–7, 2020.
- [25] W. Zhou, Y. Zhou, and J. Albert, “A true fiber-optic refractometer,” *Laser & Photonics Reviews*, vol. 11, no. 1, pp. 1–10, 2017.
- [26] A. K. Sharma, J. Gupta, and R. Basu, “Simulation and performance evaluation of fiber optic sensor for detection of hepatic malignancies in human liver tissues,” *Optics and Laser Technology*, vol. 98, pp. 291–297, 2018.
- [27] S. Wang, D. Zhang, Y. Xu, S. Sun, and X. Sun, “Refractive Index sensor based on double side-polished U-Shaped plastic optical fiber,” *Sensors 2020*, vol. 20, pp. 1–13, 2020.
- [28] M. A. Butt, S. N. Khonina, and N. L. Kazanskiy, “Silicon on silicon dioxide slot waveguide evanescent field gas absorption sensor,” *Journal of Modern Optics*, vol. 65, no. 2, pp. 174–178, 2018.
- [29] A. K. Sharma, J. Gupta, and I. Sharma, “Fiber-optic evanescent wave absorption-based sensors: A detailed review of advancements in the last decade (2007–18),” *Optik (Stuttgart)*, vol. 183, pp. 1008–1025, 2019.
- [30] D. D. Voa, R. Moradi, M. B. Gerdroodbary, and D. Ganji, “Measurement of low-pressure Knudsen force with deflection approximation for gas detection,” *Results in Physics*, vol. 13, pp. 1–6, 2019.
- [31] S. K. Gahlaut, K. Yadav, C. Sharan, and J. Singh, “Quick and selective dual mode detection of H_2S gas by mobile app employing silver nanorods array,” *Analytical Chemistry*, vol. 89, pp. 13582–13588, 2017.
- [32] P. Zaca-Morán, J. P. Padilla-Martínez, J. M. Pérez-Corte, J. A. Dávila-Pintle, J. G. Ortega-Mendoza, and N. Morales, “Etched optical fiber for measuring concentration and refractive index of sucrose solutions by evanescent waves,” *Laser Physics*, vol. 28, pp. 1–5, 2018.
- [33] Y. Cardona-Maya, A. B. Socorro, I. D. Villar, J. L. Cruz, J. M. Corres, and J. F. Botero-Cadavid, “Label-free wavelength and phase-detection based SMS fiber immune sensors optimized with cladding etching,” *Sensors and Actuators B*, vol. 265, pp. 10–19, 2018.
- [34] L. F. Rickelt, L. D. M. Ottosen, and M. Kühl, “Etching of multimode optical glass fibers: A new method for shaping the measuring tip and immobilization of indicator dyes in recessed fiber-optic microprobes,” *Sensors and Actuators B*, vol. 211, pp. 462–468, 2015.
- [35] R. X. Tan, M. Ibsen, and S. C. Tjin, “Optical fiber refractometer based metal ion sensors,” *Chemosensors*, vol. 7, no. 63, pp. 1–19, 2019.